Proceedings of the ASME 2011 International Mechanical Engineering Congress & Exposition
IMECE2011
November 11-17, 2011, Denver, Colorado, USA

IMECE2011-65387

UNIFIED CREEP PLASTICITY DAMAGE (UCPD) MODEL FOR SOLDER

Michael Neilsen
Sandia National Laboratories
Albuquerque, NM, USA

Paul Vianco
Sandia National Laboratories
Albuquerque, NM, USA

ABSTRACT

A unified creep plasticity damage (UCPD) model for Sn-Pb and Pb-free solders was developed and implemented into finite element analysis codes. The new model will be described along with the relationship between the model's damage evolution equation and an empirical Coffin-Manson relationship for solder fatigue. Next, two significant developments were needed to model crack initiation and growth in solder joints. First, an ability to accelerate the simulations such that the effects of hundreds or thousands of thermal cycles could be modeled in a reasonable amount of time was needed. This was accomplished by applying a user prescribed acceleration factor to the damage evolution; then, damage generated by an acceleration factor of cycles could be captured by the numerical simulation of a single thermal cycle. Second, an ability to capture the geometric effects of crack initiation and growth was needed. This was accomplished by replacing material in finite elements that had met the cracking failure criterion with very flexible elastic material. This diffuse crack modeling approach with local finite elements is known to generate mesh dependent solutions. However, introduction of an element size dependent term into the damage evolution equation was found to be effective in controlling mesh dependency. Finally, experimentally observed cracks in a typical solder joint subjected to thermal mechanical fatigue are compared with model predictions.

INTRODUCTION

Current approaches [e.g. 1-3] for modeling eutectic Sn-Pb solder joint response to thermal mechanical fatigue include: 1. generating finite element models of components with intact solder joints, 2. subjecting these models to one or a few thermal cycles, and 3. generating lifetime predictions based on some failure criterion. These approaches do a good job of predicting when cracks will be initiated in a solder joint; however, these approaches do not address the more important question of how many cycles will be needed to generate an electrical failure (typically an electrical open).

There are two major challenges that must be faced when we contemplate modeling cracking and predicting cycles needed to generate electrical opens in solder joints. First, cracks typically start after hundreds or more likely thousands of thermal cycles. Hundreds or thousands more cycles are needed to propagate the cracks and generate electrical opens. Adequately refined finite element models of typical components and solder joints will include thousands or millions of elements so with our current computational capabilities we are limited to modeling only a few or perhaps as many as 100 thermal cycles. Thus, a way to capture the effects of thousands of cycles in a simulation that includes only 10s of cycles is needed. Second, when a crack does occur, the boundary value problem changes. Thus, a way to automatically modify the mesh to include cracks as cracking occurs is needed.

Towashirporn et al. [4] developed a model for fatigue fracture simulations based on the use of cohesive zone elements. With their approach, failure of cohesive zone elements is based on damage in neighboring continuum elements reaching a critical value. Bhate [5] developed a similar cohesive zone element based approach. Ladani and Dasgupta [6] developed a successive-initiation strategy to model both crack initiation and growth in solder joints. With their approach, a single thermal cycle is simulated and cycles to failure predictions are generated for all elements in the solder joint. The analysis is then stepped ahead a specified number of cycles such that a small number of elements in the solder joint have failed and are removed from the simulation. A second thermal cycle is then simulated and the process is repeated until an electrical open has been generated in the solder joint.

This paper describes a different strategy to model cracking in solder joints subjected to thermal mechanical fatigue. This paper includes a description of this new strategy and the assumptions used in the development of this new capability.

Finally, experimentally observed cracks in a typical solder joint subjected to thermal mechanical fatigue are compared with model predictions.

UCPD MODEL FOR SOLDER

Unified creep-plasticity (UCP) and unified creep plasticity damage (UCPD) constitutive models for solders have been previously developed by a number of researchers [e.g. 7-13]. The UCPD model developed here is based on the UCP model developed by Boyce et al. [13]. For small elastic strains, the total strain rate, $\dot{\boldsymbol{\varepsilon}}$, can be additively decomposed into elastic, $\dot{\boldsymbol{\varepsilon}}^{e}$, and inelastic (creep + plastic), $\dot{\boldsymbol{\varepsilon}}^{in}$, parts as follows

$$\dot{\boldsymbol{\varepsilon}} = \dot{\boldsymbol{\varepsilon}}^{e} + \dot{\boldsymbol{\varepsilon}}^{in} \tag{1}$$

It is also assumed that the elastic response is linear and isotropic such that the stress rate is given by the following equation

$$\dot{\boldsymbol{\sigma}} = \mathbf{E} : \dot{\boldsymbol{\varepsilon}}^{e} = \mathbf{E} : (\dot{\boldsymbol{\varepsilon}} - \dot{\boldsymbol{\varepsilon}}^{in}) \tag{2}$$

where **E** is the fourth-order isotropic elasticity tensor. A kinetic equation for the inelastic strain rate, $\dot{\boldsymbol{\varepsilon}}^{in}$, with the following form is used:

$$\dot{\boldsymbol{\varepsilon}}^{in} = \frac{3}{2}\dot{\gamma}\,\mathbf{n} = \frac{3}{2} f \,\sinh^{p}\left(\frac{\tau}{D(1-cw)}\right)\mathbf{n} \tag{3}$$

where f is a (typically Arrhenius) function of temperature, D an internal state variable which accounts for isotropic hardening and recovery, p and c are material parameters, w is a scalar measure of damage. Note in the previous equations that damage is assumed to affect only the strength of the solder and not the elastic stiffness. **n** is the normalized stress difference tensor which is given by,

$$\mathbf{n} = \frac{\mathbf{s} - \frac{2}{3}\mathbf{B}}{\tau} \tag{4}$$

where **s** is the stress deviator, **B** is the second-order state tensor which accounts for kinematic hardening and recovery, and τ is a scalar measure of the stress difference magnitude as follows

$$\tau = \sqrt{\frac{3}{2}\left(\mathbf{s} - \frac{2}{3}\mathbf{B}\right) : \left(\mathbf{s} - \frac{2}{3}\mathbf{B}\right)} \tag{5}$$

Competing non-linear hardening and thermal recovery mechanisms are captured by the evolution equations for the internal state variable D and the internal state tensor **B**. Evolution of the internal state variable D is given by the following equation which describes competing power-law hardening and thermal or static recovery

$$\dot{D} = \frac{A_1 \dot{\gamma}}{(D - D_0)^{A_3}} - A_2 (D - D_0)^2 \tag{6}$$

where D_0, A_1, A_2, and A_3 are material parameters. Evolution of the second-order state tensor **B** is given by

$$\dot{\mathbf{B}} = \frac{A_4 \dot{\boldsymbol{\varepsilon}}^{in}}{b^{A_6}} - A_5 b \mathbf{B} \tag{7}$$

where A_4, A_5, and A_6 are material parameters and b is the magnitude of **B** as follows

$$b = \sqrt{\frac{2}{3}\mathbf{B} : \mathbf{B}} \tag{8}$$

Our previous approach for generating thermal-mechanical fatigue lifetime predictions included subjecting an intact solder joint to one or a few thermal cycles and then using equivalent plastic strain increment per cycle in the worst solder element to generate a lifetime (cycles to initiate a crack in the solder joint) prediction. With Solomon's [14] Coffin Manson failure criterion, cycles to failure, N_f, is based on the plastic shear strain range, $\Delta\gamma_p$, which for a general loading case can be related to the increment in equivalent plastic strain from one complete thermal cycle, $\Delta\gamma_{EQPS}$, to predict cycles to fatigue failure as follows

$$N_f = \left(\frac{1.14}{\Delta\gamma_p}\right)^{\frac{1}{0.51}} \approx \left(\frac{1.31636}{\Delta\gamma_{EQPS}}\right)^{1.96078} \tag{9}$$

If we assume that the damage at the end of one cycle, Δw, is simply equal to the inverse of the predicted Coffin-Manson cycles to failure we obtain

$$\Delta w = \frac{1}{N_f} = \left(\frac{\Delta\gamma_{EQPS}}{a}\right)^{b} = \left(\frac{\Delta\gamma_{EQPS}}{1.31636}\right)^{1.96078} \tag{10}$$

By differentiating this equation with respect to time, we obtain the following expression for damage rate

$$\dot{w} = \frac{b}{a^{b}}\left(\Delta\gamma_{EQPS}\right)^{(b-1)}\dot{\gamma} \tag{11}$$

This equation indicates that the damage rate depends not only on the current inelastic strain rate but also on the equivalent plastic strain that has accumulated during this cycle.

Selection of material parameters for a unified creep-plasticity damage model can be quite complex [11]. Parameters for eutectic Sn-Pb solder were obtained from a non-linear least squares fit to the normalized and aged, uniaxial tension data from Boyce et al. [13] shown in Figure 1. The non-linear least squares fit to this data was performed using the Levenberg and Marquardt Nonlinear Least Squares Algorithm [15] and a driver program for the constitutive model. Material parameters obtained from the non-linear least squares fitting process are summarized in Table 1. Since, the uniaxial tension data was monotonic, separation of kinematic hardening and recovery from isotropic hardening and recovery was not possible. For the fits tabulated here, purely isotropic hardening and recovery was assumed. Also, negligible damage is generated during the uniaxial tension tests to a strain of 5 percent; thus, the damage parameters could not be obtained from these experiments.

The uniaxial tension experiments were then simulated using the UCPD model with the material parameters summarized in Table 1. The UCPD model was able to capture the solder response over a temperature range of -60 to 100 °C and an applied strain rate range of 0.0002 s^{-1} to 200 s^{-1} (Figure 1). Damage parameters *a* and *b* were based on Solomon's [16] Coffin-Manson parameters for eutectic Sn-Pb solder. Damage parameter *c* was chosen to capture the reduction in load carrying capacity measured during a simple shear test (Figure 2) in which a copper ring was soldered to a copper plug and the resulting 0.254 mm thick solder joint was subjected to an engineering strain of +/- 5 percent at room temperature. Additional cyclic shear tests are currently in progress to further evaluate the accuracy of the models damage evolution equation.

Table 1. *UCP material parameters for Sn63-Pb37 solder.*

Temperature (°C)	-60.0	21.0	100.0
Young's Modulus (MPa)	48,276	43,255	36,860
Poisson's Ratio	0.38	0.39	0.40
Thermal Exp. Coef. (1/°C)	25.0×10^{-6}		
Flow Rate, f	4.14×10^{-20}	1.88×10^{-9}	2.21×10^{-5}
Sinh Exponent p	7.1778	4.2074	3.7151
A_1 (MPa^{A3+1})	270.67	193.44	167.76
A_2 (1/MPa-sec)	0.378×10^{-3}	1.81×10^{-3}	8.31×10^{-3}
A_3	0.970	0.970	0.970
A_4 (MPa^{A6+1})	0.0		
A_5 1/(MPa-sec)	0.0		
A_6	0.0		
Flow Stress D_0 (MPa)	8.2759		
Damage Parameter - a	1.31636		
Damage Parameter – b	1.96078		
Damage Parameter - c	0.500		

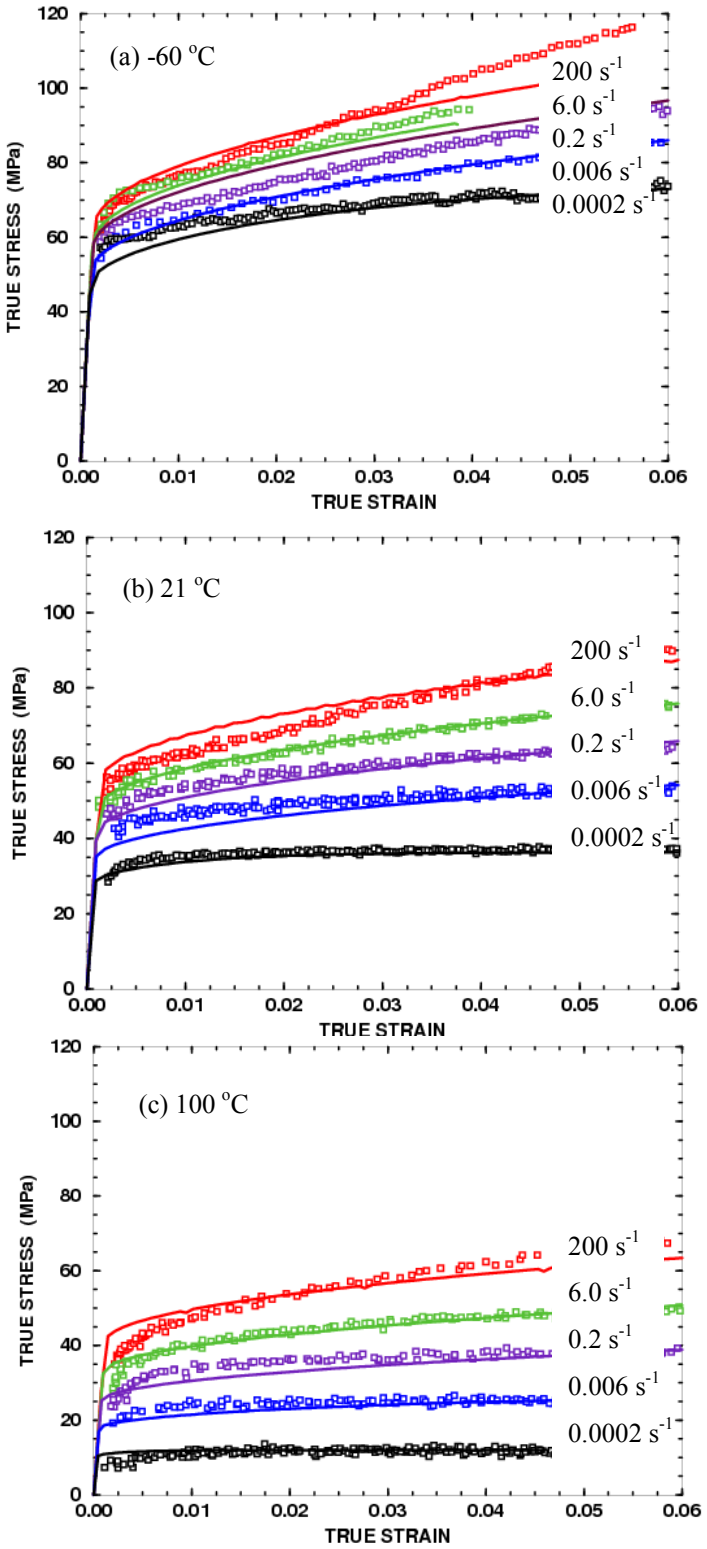

Figure 1. *Comparison of uniaxial tension test UCPD model predictions (solid lines) with experimental data (symbols). Numbers in figure represent nominal engineering strain rates.*

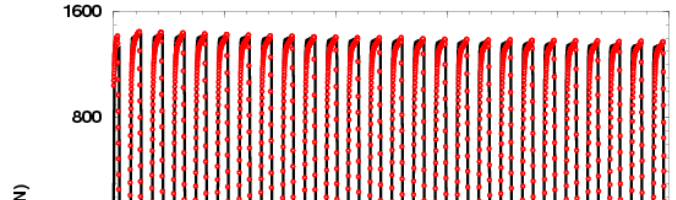

Figure 2. *Cyclic simple shear UCPD model predictions (black solid lines) compared with experimental data (red symbols).*

NEW CAPABILITY TO MODEL CRACKS IN SOLDER

The first challenge that must be faced in developing a capability to model cracking in solder joints is an ability to accelerate the simulations such that the effects of thousands of thermal cycles can be represented by simulations of only 10 or perhaps 100 cycles. Consider the typical surface mount solder joint for the small blue resistor on the validation board shown in Figure 3. This finite element model has symmetry planes on the front and left faces. Solder was modeled using the UCPD model described in the previous section and all other materials were modeled as isotropic, linear elastic with the properties listed in Table 2. If we subject this model to the temperature history shown in Figure 4, we find that the strain rate history generated in the solder joint (Figure 5) will tend to stabilize after only one or a very few number of cycles. This rapid stabilization of the strain rate history indicates that the equivalent plastic strain increment per cycle and thus the damage increment per cycle will be nearly constant.

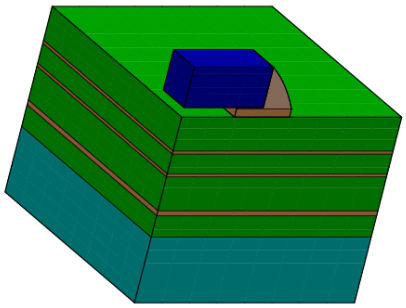

Figure 3. *Finite element model of one-fourth of the small blue resistor on multilayer printed wiring board.*

Table 2. *Material parameters for elastic materials.*

Material	Young's Modulus (MPa)	Poisson's Ratio	Thermal Expansion Coefficient ($1/^{o}C$)
Copper Pads	117,240	0.30	17.0×10^{-6}
Alumina Ceramic	275,860	0.21	6.0×10^{-6}
BT Laminate PWB	23,100	0.18	14.0×10^{-6}
Duroid PWB	2,069	0.18	19.5×10^{-6}

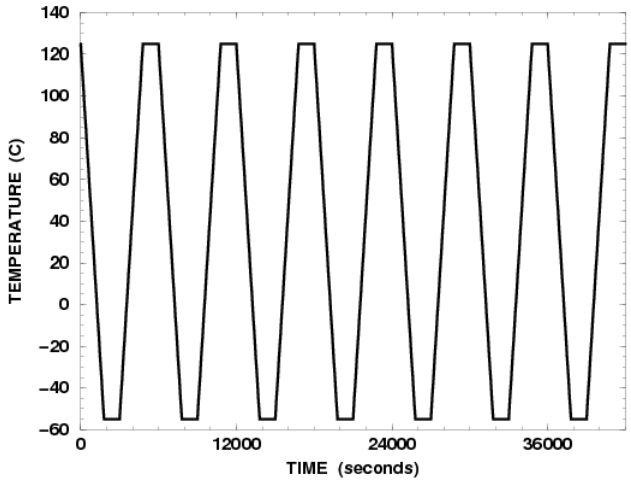

Figure 4. *Temperature history used for simulation.*

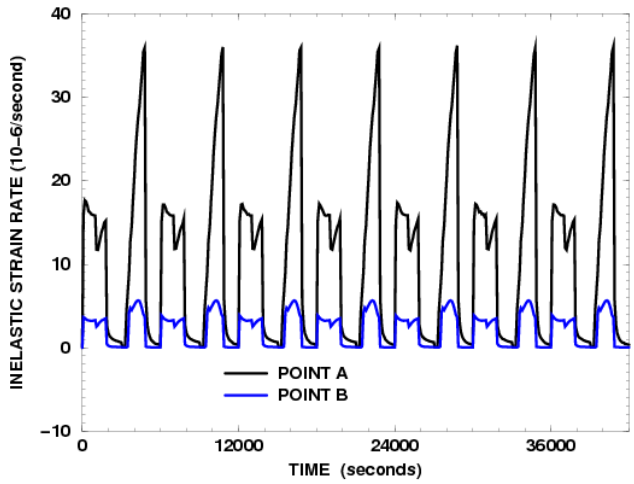

Figure 5. *Inelastic strain rate history at Points A and B (see Figure 7a for Point locations) in the solder joint.*

Thus, the damage generated by an acceleration factor, *F*, number of cycles can be captured by simulating a single cycle

and applying the acceleration factor to the damage evolution equation as follows

$$\dot{w} = F \frac{b}{a^b} \left(\Delta\gamma_{EQPS} \right)^{(b-1)} \dot{\gamma} \qquad (12)$$

This is analogous to the approach used by Towashiraporn et al. [4] in which the disturbance state is extrapolated using a one-term Taylor expansion to make the fatigue modeling computationally tractable.

To show that this simulation acceleration works as expected, the small blue resistor in Figure 3 was analyzed using 3 different acceleration factors, 1, 10, and 250. Results from these simulations showed that damage history predicted at two different locations in the solder joint would be nearly identical with the three different acceleration factors applied to the simulations (Figure 6). Note that in the model, damage is not allowed to increase beyond a maximum value of 0.90. Contour plots of damage after 500 cycles are compared for the 3 different acceleration factors in Figure 7. Note that the contour plots are very similar. The only significant difference between these analyses is the amount of computational effort required to obtain the results. The simulation with an acceleration factor of 1 required the simulation of all cycles and took about 186,000 CPU seconds to get to 500 cycles; however, the simulation with an acceleration factor of 250 required the simulation of only 2 cycles to represent 500 actual cycles and took only 760 CPU seconds to get to 500 cycles.

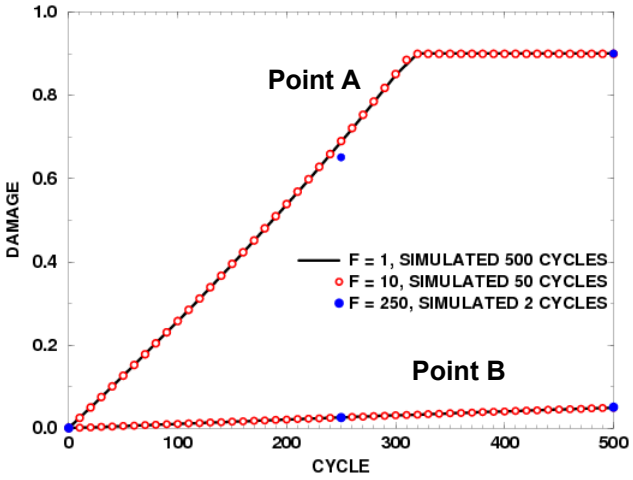

Figure 6. *Damage predicted at two different locations in solder joint with acceleration factors of 1, 10, and 250. Locations of Points A and B are shown in Figure 7a.*

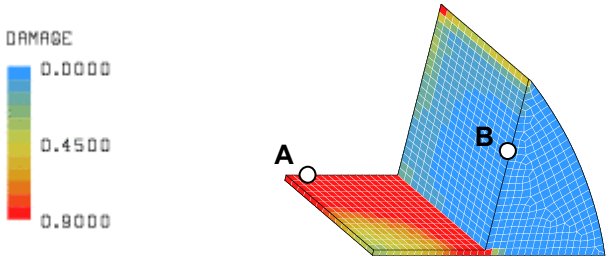

(a) F = 1, simulated 500 cycles

(b) F =10, simulated 50 cycles

(c) F = 250, simulated 2 cycles

Figure 7. *Contour plots of damage in the solder joint after 500 thermal cycles.*

The next step was to develop a capability to model solder joint cracks. Since solder joint cracks are typically rather diffuse (not a single crack with a sharp crack tip), a simple smeared crack modeling approach was used. When damage reached a critical level (w_{fail} = 0.9 for these simulations), the constitutive response of the solder material was changed to be that of a weak (very flexible) elastic material as follows

$$Is\ w \geq w_{fail} \begin{cases} Yes \rightarrow & \boldsymbol{\sigma} = 0.001\ \mathbf{E} : \boldsymbol{\varepsilon} \\ No \rightarrow & \text{use UCPD model} \end{cases} \qquad (13)$$

Once the material is cracked, it is not allowed to change back to an uncracked material.

EFFEECT OF MESH SIZE ON PREDICTIONS

The effects of mesh refinement on lifetime predictions were studied using the finite element models with widely varying mesh refinement shown in Figure 8. In Figure 8, variable *LIFE* was plotted when cracks were initiated under the resistor, and when an electrical open was first generated. *LIFE* is given by the following equation

$$LIFE = \frac{w}{w_{fail}} = \frac{w}{0.9} \qquad (14)$$

LIFE is 0 for undamaged solder and equal to 1 for solder that has cracked Thus, white elements in Figure 8 represent elements that have *LIFE* equal to one and have cracked.

Figure 8 shows that the predicted cycles to initiate a crack decreased from 3,300 cycles for the very coarse mesh to 600 cycles for the most refined mesh. The predicted cycles to generate an electrical open decreased from 33,600 cycles with the very coarse mesh to 10,050 cycles when the solder element edge length was decreased by a factor of 8.

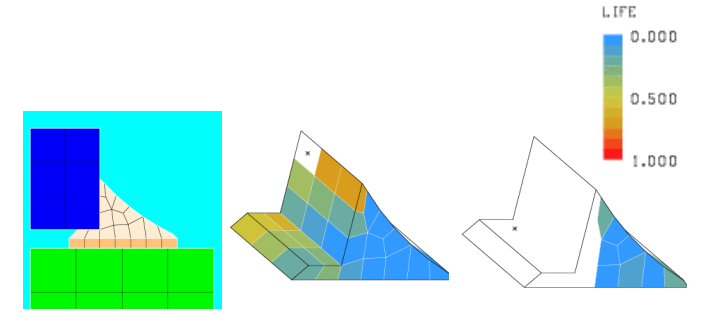

(a) 42 solder element 3,300 cycles 33,600 cycles

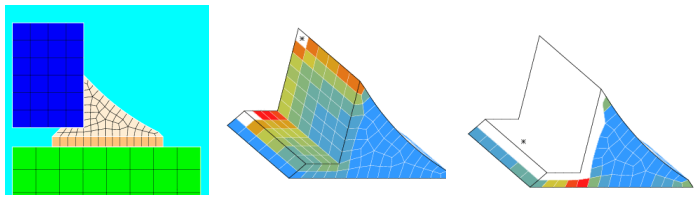

(b) 318 solder elements 2,250 cycles 19,650 cycles

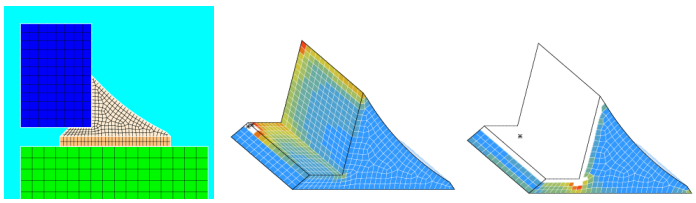

(c) 2,782 solder elements 1,050 cycles 14,400 cycles

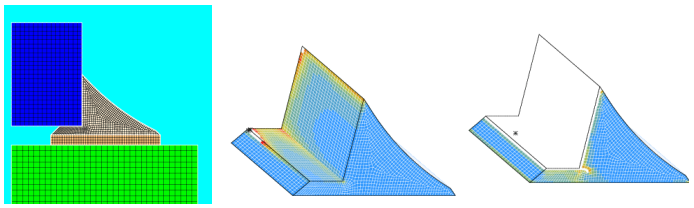

(d) 22,152 solder elements 600 cycles 10,050 cycles

Figure 8. *Local model predictions for cycles needed to initiate and grow cracks to failure (electrical open) are mesh dependent.*

One approach for dealing with the mesh dependency would be to develop a non-local model. An alternate approach would be to simply have the damage rate depend on the element size as follows

$$\dot{w} = \left(\frac{V^{1/3}}{\lambda}\right)^{d} F \frac{b}{a^{b}} \left(\Delta\gamma_{EQPS}\right)^{(b-1)} \dot{\gamma} \qquad (15)$$

where V is the element volume and raised to the 1/3 power which gives the element edge length for a cube, and λ is a characteristic length, and d a material parameter. The previous mesh refinement study was repeated using Equation 15 for the damage evolution and, λ = 0.0254 mm, d = 0.61 (Figure 9). The predictions are significantly less mesh dependent by having the damage rate depend on element size.

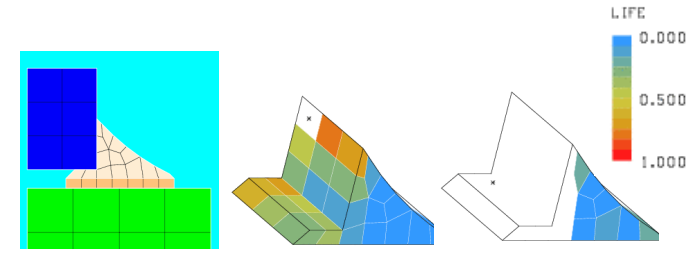

(a) 42 solder element 1,200 cycles 9,900 cycles

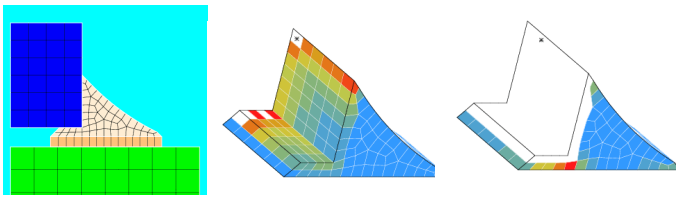

(b) 318 solder elements 1,200 cycles 9,450 cycles

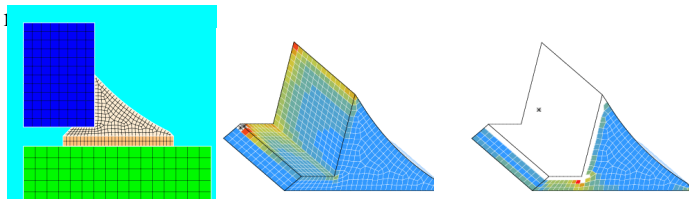

(c) 2,782 solder elements 900 cycles 10,200 cycles

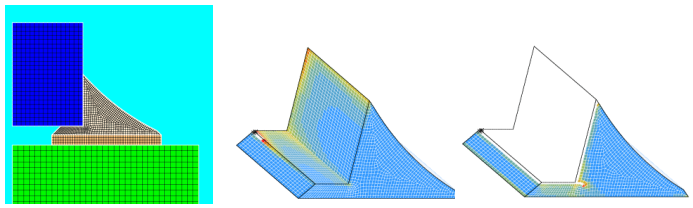

(d) 22,152 solder elements 600 cycles 10,500 cycles

Figure 9. *Element size dependent model predicted cycles needed to initiate and grow cracks to failure (electrical open).*

COMPARISON WITH EXPERIMENTS

Experimental observations of cracking in the small blue resistor indicated that cracking would start under the resistor

(Figure 10) and then a second crack would start near the outer upper corner. Cracking simulations with the new UCPD solder model predicted cracks starting under the resistor, followed by cracks starting near the upper outer corner (note that in the model images the front face is a symmetry plane, a mid-surface, and in the first two experimental images, Figure 10a and 10b, below the front face is an outer surface). The UCPD model predicts the correct starting location and propagation of the experimentally observed cracks. In these simulations, when a damage failure value, w_f, of 0.9 was used, the crack progression at 500, 1000, and 1500 cycles appears to be in good agreement with experimental observations (Figure 10).

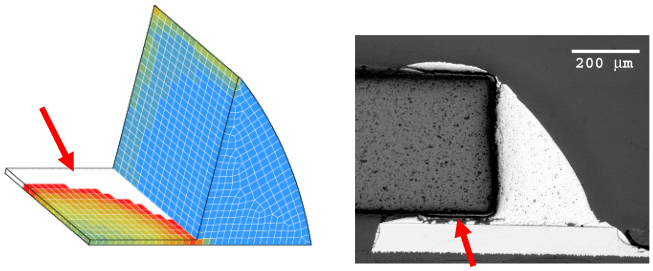

(a) 500 cycles (crack under resistor)

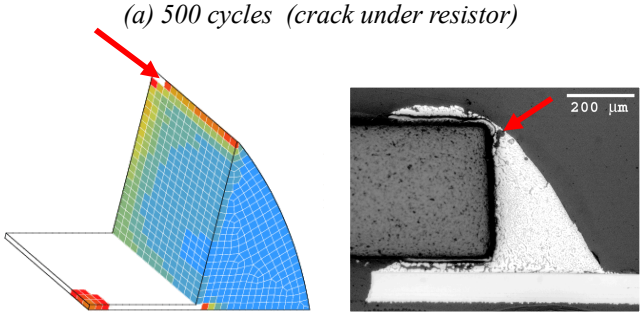

(b) 1000 cycles (crack starts near upper outer corner)

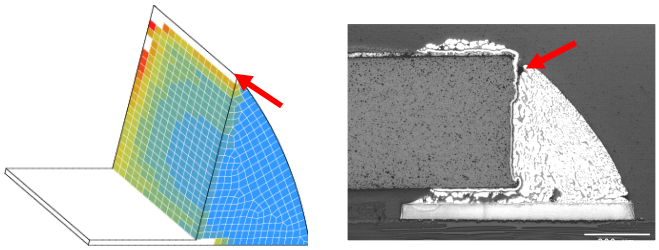

(c) 1500 cycles (upper crack propagated to mid-plane)

Figure 10. *Contour plots of solder life for simulations with a failure value, w_f = 0.9, and an acceleration factor of 250 compared with experimental observations of cracking. White elements in the simulation represent elements that have cracked.*

SUMMARY

A new capability for modeling cracking in solder joints subjected to thermal-mechanical fatigue was developed. This capability is based on: 1. acceleration of the simulations with an acceleration factor built into the constitutive routine, 2. a smeared cracking approach that changes the constitutive response of the solder to a weak (very flexible) elastic material when the failure criterion has been met, and 3. control of mesh dependency with a damage evolution that is dependent on the element volume. The predicted cycles to generate an electrical open are insensitive to mesh refinement. The predicted cycles to initiate a crack still show some sensitivity to mesh refinement, so care must be taken to ensure that the mesh refinement used in applications is consistent with mesh refinement used for validation. This new capability does an excellent job of balancing prediction accuracy with computational effort required to achieve that accuracy.

Currently, the new capability is implemented in finite element codes developed at Sandia National Laboratories. Next steps will include: 1. completion of additional comparisons with fatigue experiments, 2. completion of validation simulations with the new capability on a variety of component/solder joint types, and 3. development of a similar capability, parameters for Pb-free solders.

ACKNOWLEDGMENTS

The experimental uniaxial tension data provided by Brad Boyce, Sandia National Laboratories, and the fatigue data provided by J. Mark Grazier,, Sandia National Laboratories, was essential for the UCPD model development presented in this paper. Sandia is a multi-program laboratory operated by Sandia Corporation, a Lockheed Martin Company, for the United States Department of Energy's National Nuclear Security Administration under contract DE-AC04-94AL85000.

REFERENCES

[1] Perkins, A.E., and Sitaraman, S.K., **Solder Joint Reliablity Predictions for Multiple Environments**, Springer, 2009.

[2] Zhang, Q., and Dasgupta, A., 'Systematic Study on Thermo-Mechanical Durability of Pb-Free Assemblies: Experiments and FE Analysis,' ASME J. Electron. Packag., Vol. 127, 2005.

[3] Darveaux, R., 2002, 'Effect of Simulation Methodology on Solder Joint Crack Growth Correlation and Fatigue Life Prediction,' ASME J. Electron. Packaging, Vol. 124, 2002.

[4] Towashiraporn, P., Subbarayan, G. S., and Desai, C. S., 'A Hybrid Model for Computationally Efficient Fatigue Fracture Simulations at Microelectronic Assembly Interfaces,' Int. J. Solids Struct., Vol. 42, pp. 4468–4483, 2005.

[5] Bhate, D., Chan, D., Subbarayan, G., and Nguyen, L., 'A Nonlinear Fracture Mechanics Approach to Modeling Fatigue

Crack Growth in Solder Joints,' ASME J. Electron. Packaging, Vol. 130, 2008.

[6] Ladani, L.J. and Dasgupta,A., 'Damage Initiation and Propagation in Voided Joints: Modeling and Experiment,' Journal of Electronic Packaging, Vol. 130, March 2008.

[7] Anand, L., "Constitutive Equations for Hot-Working of Metals," International Journal of Plasticity, 1(3), pp. 213-231, 1985.

[8] Busso, E. P., Kitano, M., and Kumazawa, T., "A Visco-Plastic Constitutive Model for 60/40 Tin-Lead Solder Used in Ic Package Joints," Transactions of the ASME. Journal of Engineering Materials and Technology, 114(3), pp. 331-7, 1992.

[9] Frear, D.R., Burchett, S.N., Neilsen, M.K., and Stephens, J.J., 'Microstructurally Based Finite Element Simulation of Solder Joint Behaviour,' *Soldering and Surface Mount Technology*, No. 25, pp. 39-42, February 1997.

[10] Nose, H., Sakane, M., Tsukada, Y., and Nishimura, H., "Temperature and Strain Rate Effects on Tensile Strength and Inelastic Constitutive Relationship of Sn-Pb Solders," Journal of Electronic Packaging, 125(1), pp. 59-66, 2003.

[11] Fossum, A. F., Vianco, P. T., Neilsen, M. K., and Pierce, D. M., "A Practical Viscoplastic Damage Model for Lead-Free Solder," Journal of Electronic Packaging, 128(1), pp. 71-81, 2006.

[12] Ohguchi, K. I., Sasaki, K., and Ishibashi, M.,'A Quantitative Evaluation of Time-Independent and Time-Dependent Deformations of Lead-Free and Lead-Containing Solder Alloys,' Journal of Electronic Materials, 35(1), pp. 132-9, 2006.

[13] Boyce, G.L., Brewer, L.N., Neilsen, M.K, and Perricone, M.J., 'On the Strain Rate and Temperature Dependent Tensile Behavior of Eutectic Sn-Pb Solder,' Journal of Electronic Packaging, accepted for publication, 2011.

[14] Solomon, H.D. 'Fatigue of 60/40 Solder,' IEEE Trans. on Components, Hybrids, and Manuf. Tech., Vol. 9, No. 4, December 1986.

[15] More, J. J., 'The Levenberg-Marquardt Algorithm: Implementation and Theory,' Proceedings of the Biennial Conference on numerical analysis, pp. 105-16., 1978